Experimental and kinetic study on the laminar flame propagation of cyclopentanone at elevated pressures: understanding its flame chemistry and comparison with cyclopentane and cyclopentanol

Qiying Zhang, Jun Fang, Qilong Fang and Wei Li*

Institute of Aerospace Propulsion, School of Mechanical Engineering, Shanghai Jiao Tong University, Shanghai 200240, PR China
* Corresponding author, E-mail: lw2017@sjtu.edu.cn

Abstract

Cyclopentanone, a promising clean alternative fuel derived from biomass, was investigated in this work for its laminar burning velocities (LBVs). Experiments were conducted in a constant-volume cylindrical combustion vessel under an initial temperature of 443 K, initial pressures of 1 to 5 atm, and equivalence ratios ranging from 0.6 to 1.5 using high-pressure. The newly obtained experimental data were used to validate three representative kinetic models of cyclopentanone combustion from the literature. Among them, the Li model (Energy Fuels, 2021, 35: 14023–143034) provided the most accurate predictions of the experimental data. Based on the Li model, kinetic analyses incorporating sensitivity analysis and rate of production analysis were conducted to systematically investigate the effects of equivalence ratio and pressure on the LBVs of cyclopentanone. The results indicate that vinyl-related reactions play significant roles in cyclopentanone flames, with $C_2H_3 + H = C_2H_2 + H_2$ being the most critical inhibiting reaction under rich conditions. With the increase of the initial pressure, the sensitivity coefficient of $H + O_2 (+ M) = HO_2 (+ M)$ gradually increases and exceeds $C_2H_3 + H = C_2H_2 + H_2$ under equivalent conditions. Furthermore, a comparison of LBVs with those of cyclopentane and cyclopentanol—both compounds with similar five-membered ring structures—shows that cyclopentanone exhibits significantly faster flame propagation. This behavior is mainly attributed to the unique molecular structure of cyclopentanone, which facilitates the generation of reactive radicals such as C_2H_3 and H during the combustion process, effectively promoting its flame propagation.

Introduction

Cyclopentanone is a highly promising clean alternative fuel that can be extensively derived from biomass. Recent studies have demonstrated that selective catalytic conversion of lignocellulosic-derived furfural facilitates the efficient production of cyclopentanone at a relatively low economic cost[1]. The application of cyclopentanone as a substitute for fossil fuels in practical combustion systems has demonstrated significant potential for reducing carbon emissions. Additionally, cyclopentanone contains a carbonyl functional group, which significantly mitigates the soot produced during combustion[2,3]. Tong et al.[4] investigated the combustion characteristics of cyclopentanone/diesel blends in engines, revealing that the incorporation of cyclopentanone extends the ignition delay time (IDT) and increases the peak combustion temperature within the cylinder. Furthermore, compared to pure diesel, cyclopentanone blends significantly reduced particulate matter emissions.

Several studies have explored the fundamental combustion characteristics and kinetic modeling of cyclopentanone, including LBVs, IDTs, and the concentrations of pyrolysis/oxidation components. The LBV is a critical parameter for assessing the gas-phase diffusion and reactivity within combustion systems, as well as for validating the overall performance of kinetic models. Bao et al.[5] measured the LBV of cyclopentanone at 1 atm and under varying initial temperatures (T_u = 423, 448, and 473 K) in a constant-volume combustion chamber. Their results indicate that the laminar flame propagation of cyclopentanone is comparable to that of ethanol and gasoline under lean conditions; however, at equivalence ratios (ϕ) from 1.0 to 1.4, The LBV of cyclopentanone exhibits an intermediate value,

positioning it between gasoline and ethanol in terms of combustion reactivity. Zhang et al.[6] conducted an experimental study of laminar flame propagation of cyclopentanone at various initial temperatures and atmospheric pressure based on the spherical flame method and heat flux method. It was also compared with ethanol and *n*-propanol to investigate the effect of the unique ring structure of cyclopentanone on the LBV. While some efforts have been made in understanding cyclopentanone's laminar flame propagation, research under elevated pressures is still limited, and the pressure effect on its flame characteristics of cyclopentanone remains unclear.

In terms of kinetic modeling, Zhang et al.[6,7] constructed a detailed chemical kinetic model for cyclopentanone, validating it with LBVs and IDTs data. Sun et al.[8] explored the species distribution of cyclopentanone laminar premixed flames and developed a kinetic model to interpret the high-temperature combustion chemistry of cyclopentanone. Additionally, Li et al.[9] from our research group conducted a comprehensive investigation of cyclopentanone in a flow reactor, employing synchrotron vacuum ultraviolet photoionization mass spectrometry (SVUV-PIMS) across a temperature range from 875 to 1,428 K and pressures from 0.04 to 1 atm. Their research included theoretical calculations of the fuel unimolecular decomposition and the construction of a detailed kinetic model. Overall, research on the fundamental combustion properties of cyclopentanone remains limited, particularly regarding experimental measurements of LBV at elevated pressures. Consequently, further experimental studies of cyclopentanone's laminar flame propagation are essential to deepen the understanding of its combustion chemistry.

In this work, the laminar flame propagation of cyclopentanone/air blends are investigated in a high-pressure cylindrical constant volume combustion vessel at a temperature of 443 K, pressures of 1, 2, and 5 atm, and equivalence ratios of 0.6 to 1.5. We evaluated three existing kinetic models against our experimental data and conducted a comprehensive kinetic analysis proposed by Li et al.[9], focusing on the effect of equivalence ratio and pressure on flame propagation. Additionally, to explore the kinetic mechanisms underlying the differences in LBVs among cyclic fuels with various functional groups, a comparison of the LBVs of cyclopentanone, cyclopentane, and cyclopentanol were conducted.

Methodology

Experimental setup

The experiments on LBV were performed in a high-pressure, constant-volume cylindrical combustion vessel at Shanghai Jiao Tong University (Shanghai, China). A schematic of the experimental setup is shown in Fig. 1, which includes the combustion vessel, the premixing vessel, the vaporizer, the pipelines, and the temperature control system[10]. The combustion vessel consists of a single-chamber cylindrical structure constructed from 304 stainless steel, featuring an internal diameter of 150 mm and a length of 152 mm. Two quartz windows with a diameter of 75 mm and a thickness of 30 mm are positioned on either side of the vessel, allowing imaging of the flame propagation process. The combustion vessel is heated to 443 K using a heating jacket, with the temperature monitored and regulated by a K-type thermocouple and a PID temperature controller. The ignition of the combustible mixture is facilitated by a pair of horizontally aligned tungsten electrodes, each with a diameter of 500 μm positioned at the center of the vessel. Flame propagation is recorded at 12,000 fps by a Schlieren system with a high-speed camera. The LBVs and Markstein lengths are subsequently

extracted from the recorded flame images through established data processing methods described in previous work[10].

Data processing

In the LBV experiments, flame images were captured by a high-speed camera. The stretched flame speed is determined through the differential calculation of the flame radius:

$$S_b = \frac{dr_f}{dt} \tag{1}$$

where, r_f is the radius of the flame surface, t is the elapsed time after ignition, and b refers to the unburned state. The stretch rate of the spherical flame is defined as:

$$\kappa = \frac{dlnA_f}{dt} = \frac{2}{r_f}\frac{dr_f}{dt} \tag{2}$$

where, κ is the flame stretching rate, and A_f is the area of the spherical flame surface. Subsequently, the LBV of the unstretched flame can be obtained from the nonlinear relationship[11]:

$$\left(\frac{S_b}{S_b^0}\right)^2 ln\left(\frac{S_b}{S_b^0}\right)^2 = -\frac{2L_b\kappa}{S_b^0} \tag{3}$$

where, S_b^0 represents the unstretched flame speed, while L_b denotes the Markstein length. After obtaining the unstretched flame LBV of the burned gas, the unstretched flame velocity and Markstein length in the unburned state can be obtained by dividing the nonlinear regression results by the density ratio:

$$S_u^0 = \frac{S_b^0}{\sigma} = \frac{\rho_b^0 S_b^0}{\rho_u^0} \tag{4}$$

where, S_u^0 is the unstretched LBV, density ratios (ρ_b^0/ρ_u^0) were calculated by Chemkin-Pro software[12].

The uncertainty of the data for LBV is comprehensively evaluated and presented in detail in our previous work[10]. The total uncertainty of LBVs involves a combination of extrapolation methods, experimental repeatability, buoyancy effects, radiation effects, and
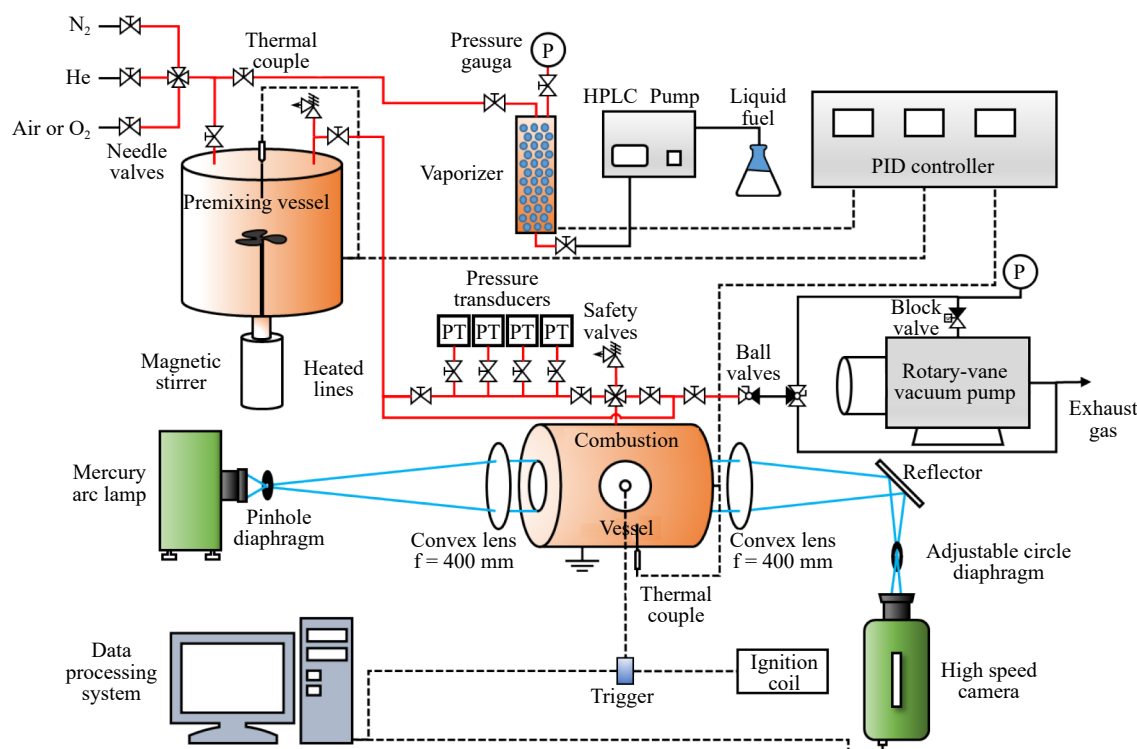

Fig. 1 A schematic constant-volume combustion vessel[10].

density ratios. Specifically, the empirical formula proposed by Yu et al.[13] is adopted to quantify the uncertainty in LBV caused by the radiation effect, as follows:

$$B_{rad,rel} = \frac{S^0_{u,RCFS} - S^0_{u,Exp}}{S^0_{u,Exp}} = 0.82 \left(\frac{S^0_{u,Exp}}{S_0} \right)^{-1.14} \left(\frac{T_u}{T_0} \right) \left(\frac{P}{P_0} \right)^{-0.3} \quad (5)$$

where, $S^0_{u,RCFS}$ is the radiation corrected burning velocity, $S^0_{u,Exp}$ is the measured LBV for spherical flame, reference conditions are: $S_0 = 1$ cm/s, $T_0 = 298$ K, $P_0 = 1$ atm. The offset of the flame center reflects the buoyancy effect. A fitting method from de Vries et al.[14] is used to get the center of the spherical flame. The contribution of buoyancy to the relative uncertainty of LBV is quantified using Eqn (6).

$$B_{buo,rel} = \frac{s_{b,buo} - S_b}{s_b} = \frac{d(\delta r_f)}{dr_f} \quad (6)$$

where, r_f and $r_f + \delta r_f$ are the ideal flame radius and buoyancy-affected flame radius respectively, $s_{b,buo} = d(r_f + \delta r_f)/dt$ is the buoyancy-affected s_b. The deviation of density ratio arises from the simplification of the physical model and it is evaluated by Eqn (7),

$$B_{\sigma sim,rel} = \frac{\sigma_{S_L} - \sigma_{Eq}}{\sigma_{Eq}} \quad (7)$$

where, σ_{Eq} is the density ratio calculated by equilibrium, σ_{S_L} is the density ratio calculated by premixed flame, and $B_{\sigma sim,rel}$ is the relevant difference between the two methods. In this work, each experiment was conducted in triplicate to ensure reliability. The mean value of the three repetitions was used as the best estimate of the measured quantity, while the standard deviation of the repeated measurements was employed to assess random uncertainty. Following this, the relative combined overall uncertainties of the measured LBVs were determined by systematically integrating the aforementioned uncertainties. The uncertainties of LBV in this work are in the range of 1.06–1.66 cm/s.

Numerical method

In this work, three cyclopentanone kinetic models — the Sun model[8], the Zhang model[6], and the Li model[9] — were validated against the measured LBV. It should be noted that since no transport data were provided in the Li model, transport data were added to the Li model based on previous studies[15–18] to perform LBV simulations. The information on these models is shown in Table 1. Numerical modeling of the LBV was performed using CHEMKIN PRO[12] software, adopting the Premixed Laminar Flame-speed module. The maximum number of grids was set to 1,000, while the curvature parameter and the gradient parameter were set to 0.1. Additionally, multi-component transport and Soret effect were considered in the simulations.

Results and discussion

Experimental and simulated results

Figure 2 presents the measured LBVs at pressures of 1, 2 and 5 atm. As shown, at all three pressures, the LBV initially rises and subsequently declines with increasing equivalence ratio across all three pressures, with the peak occurring at $\phi = 1.1$. Under rich conditions at 5 atm, cellular instabilities tend to influence spherical

flames, causing surface wrinkling that accelerates flame propagation; thus, the maximum valid equivalence ratio under these conditions is 1.2.

The predictive performance of the three kinetic models at various pressures is also compared in Fig. 2. Under all tested conditions, the Li model reasonably predicts the experimental data for cyclopentanone. The Sun and Zhang models exhibit different prediction performances under different conditions. Specifically, at 1 atm, the Sun model significantly overestimates experimental data, while the Zhang model agrees with the experimental results only at equivalence ratios of 1.4 and 1.5, and is overestimated at other equivalence ratios. At 2 atm, the Sun model continues to overpredict the experimental data. However, the simulation results of the Zhang model produce results closer to the experimental data, with only a slight overprediction under lean conditions, suggesting that it overestimates the pressure dependence of flame propagation in cyclopentanone/air mixtures. At 5 atm, the Sun model overpredicts the experimental data across all experimental equivalence ratios. The Zhang model, on the other hand, agrees with the experimental data under lean conditions ($\phi < 1.0$), but underpredicts under rich conditions ($\phi \geq 1.0$). Based on these findings, the Li model was selected for further kinetic analysis.

The Markstein length is also an important parameter that characterizes the stability of the fuel combustion properties in the spherical flame propagation. The experimental results of Markstein length
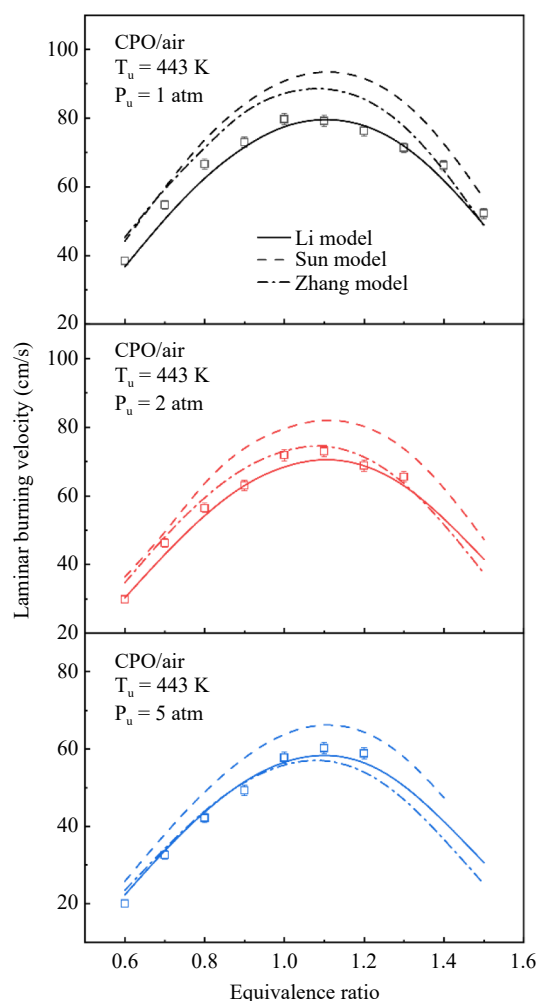

Fig. 2 Experimental and simulated LBVs of cyclopentanone/air mixtures at 443 K and 1–5 atm.

Table 1. Details of the chemical kinetic models published in literature.

Model	Year	Number of species	Number of reactions
Sun model	2018	515	2,840
Zhang model	2020	239	1,660
Li model	2021	220	1,671

at various pressures and equivalence ratios are shown in Fig. 3. The Markstein length is defined as shown in Eqn (3), which indicates the sensitivity of the LBV of the fuel mixture to the stretch rate. From Fig. 3, it can be seen that Markstein length decreases with increasing equivalence ratio for all three pressures. The lower Markstein length suggests a reduced sensitivity of LBVs to stretch rate and indicates that cellular instabilities arise at lower pressures and equivalence ratios[19]. At 1 atm, the Markstein length decreases to a negative value when the equivalence ratio is increased to 1.5. With increasing pressure, the Markstein length decreases and the cellular instability occurs at lower equivalence ratios, as a result, no valid data are available for some of the rich conditions at high pressures.

Effects on LBVs

Equivalence ratio effects

To elucidate the influence of the equivalence ratio on cyclopentanone laminar flame propagation, this study analyzes the reaction pathways of cyclopentanone/air mixtures under lean and rich conditions. Figure 4 illustrates the primary pathways of the cyclopentanone combustion at two equivalence ratios, where $\phi = 0.7$ and 1.4 represent the lean and rich conditions, respectively. It can be seen that cyclopentanone first undergoes H-abstraction with free
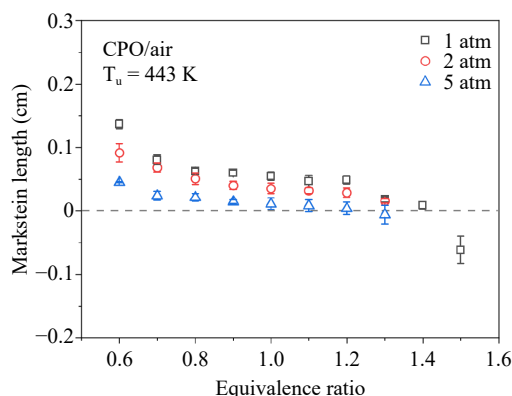
radicals to form $ACYC_5H_7O$, $BCYC_5H_7O$, and C_2H_4, respectively. Under lean conditions, 38.8% of the cyclopentanone is converted to $ACYC_5H_7O$, 12.7% to C_2H_4, and 46.0% to $BCYC_5H_7O$. For rich conditions, the contribution ratios differ slightly, with more fuel being converted to $ACYC_5H_7O$ (42.0%) and fewer to C_2H_4 (7.9%), and $BCYC_5H_7O$ (41.4%).

Subsequently, $ACYC_5H_7O$ undergoes the ring-opening reaction to produce two ketone radicals containing C=C bonds, which further eliminate CO to produce C_4H_5O radicals, followed by β-scission reactions to produce vinyl radicals. Similarly, $BCYC_5H_7O$ also undergoes the ring-opening reaction and further generates ethylene, vinyl, and allyl via α-scission or β-scission reactions. It can be found that cyclopentanone mainly generates unsaturated C_2 and C_4 species through H-abstraction, ring opening, and scission reactions, and rarely generates CH_3. Equivalence ratios have a minor effect on the reaction pathway and branching ratios, and the main reaction pathways are almost the same in both lean and rich combustion conditions.

Sensitivity analyses were performed under various equivalence ratios to investigate the effect of ϕ on flame propagation, as shown in Fig. 5. Under lean conditions, the chain-propagation reaction CO + OH = CO_2 + H and the chain-branching reaction H + O_2 = O + OH are the two most promoting reactions, with the sensitivity of the former one being slightly higher than that of the latter one. H + O_2 (+ M) = HO_2 (+ M) is the most inhibiting reaction for flame propagation. As ϕ increases, the sensitivity of H + O_2 = O + OH increases and becomes the most promoting reaction at $\phi = 1.0$ and 1.4. Meanwhile, the sensitivities of vinyl-related reactions, such as C_2H_3 + H = C_2H_2 + H_2 and C_2H_3 + O_2 = CH_2CHO + O, also exhibit a gradually increasing trend with increasing equivalence ratio. Under rich conditions, the sensitivity coefficient of C_2H_3 + H = C_2H_2 + H_2 exceeds that of H + O_2 (+ M) = HO_2 (+ M), making it the most negative reaction. This indicates that C_2H_3 plays a more important role in rich cyclopentanone flames, which is quite similar to that in ethylene flames[20]. It is also noticed that different from hydrocarbon flames[21,22] and other oxygenated fuel flames[23,24], methyl-related reactions, particularly CH_3 + H (+ M) = CH_4 (+ M), are not among the sensitive reactions because of the limited production of methyl in cyclopentanone flames. In addition, the three H-abstraction
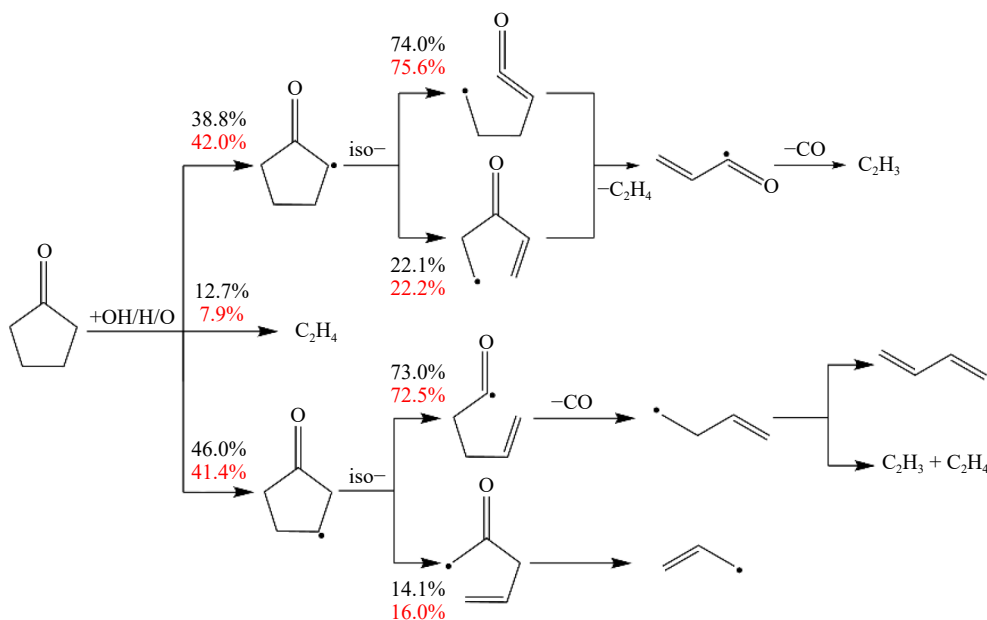

Fig. 3 Measured Markstein lengths of cyclopentanone/air flames at 443 K and 1–5 atm.

Fig. 4 Main reaction networks in cyclopentanone flame at 1 atm (black: $\phi = 0.7$, red: $\phi = 1.4$).
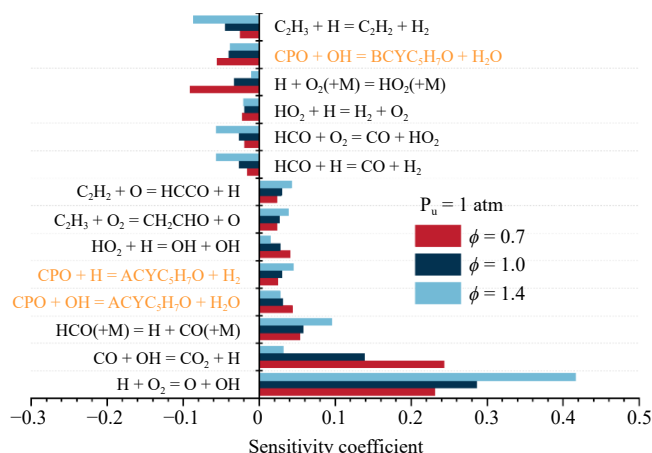
Fig. 5 Sensitivity analysis of LBV for cyclopentanone/air mixtures at 473 K, 1 atm, and various equivalence ratios.

reactions of cyclopentanone exhibit high sensitivity at various equivalence ratios, with the reactions producing $ACYC_5H_7O$ being promoting due to the large amounts of ethylene and vinyl while the reaction producing $BCYC_5H_7O$ is inhibiting due to the competition with the former.

Pressure effects

Figure 6 shows the results of LBVs of cyclopentanone/air mixtures at 1–5 atm, and the LBVs show a significant decreasing trend with the increase of the pressure. In other words, LBVs of cyclopentanone/air mixtures exhibit a clear pressure dependence. For comparison, Fig. 7 shows the variation in LBVs with the pressure under three equivalence ratios. The trend of LBVs with pressure is similar across different equivalence ratios, with all exhibiting nonlinear behaviors. Superficially, the influence of pressure on LBV diminishes as the pressure increases. Based on previous studies[25–27], the LBV is exponentially correlated with the pressure, as shown in Eqn (8):

$$S_u^0 = S_{u,0}^0 \left(\frac{P_u}{P_0}\right)^\beta \tag{8}$$

where, P_0 is the reference pressure (1 atm in this work), $S_{u,0}^0$ is the LBV at 1 atm, S_u^0 is the LBV at pressure P_u, and β is the pressure-dependent coefficient. The β is equal to $0.5n-1$, and n is the global reaction order. The pressure-dependent coefficients at various equivalence ratios are shown in Fig. 8. It is observed that as the equivalence ratio increases, the β initially rises, reaches a maximum at $\phi = 1.2$, and subsequently declines. Since β is negative, a smaller β means a stronger pressure
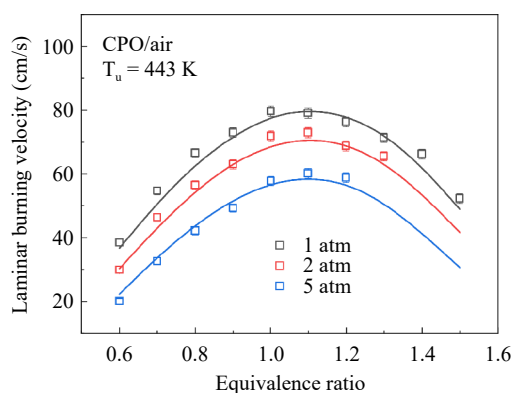
dependence of LBV. For equivalence ratios ranging from 0.6 to 1.3, the value of β varies between −0.19 and −0.41.

To further examine the chemical effect of pressure on flame propagation, sensitivity analysis at stoichiometric ratio and pressures of 1, 2, and 5 atm was performed, as shown in Fig. 9. Under the three pressure conditions, $H + O_2 = O + OH$ is the reaction with the highest positive sensitivity coefficients, which generates O and OH radicals that promote flame propagation. At 1 atm, $C_2H_3 + H = C_2H_2 + H_2$ is the most inhibiting reaction for flame propagation. As pressure increases, the sensitivity coefficient of the third-body reaction $H + O_2 (+ M) = HO_2 (+ M)$ is also enhanced, thereby inhibiting the flame propagation of the cyclopentanone. In addition, the elementary reactions associated with the initial consumption of fuel are also highly sensitive under all investigated pressures. Specifically, the H-abstraction of cyclopentanone with OH/H radicals producing $ACYC_5H_7O$ have high positive sensitivity coefficients, while H-abstraction reaction of cyclopentanone with OH producing $BCYC_5H_7O$ has the high negative sensitivity. This can be attributed to the fact that $ACYC_5H_7O$ mainly generates C_2H_4 and C_2H_3 in the subsequent decomposition reactions, which favor enhancing the flame propagation. In contrast, the reaction generating $BCYC_5H_7O$ competed with the above reactions for reactive radicals, thereby inhibiting the flame propagation.

Fuel molecular structure effects: comparison with cyclopentane and cyclopentanol

Similar to cyclopentanone, cyclopentanol is a fine chemical f eedstock that can be obtained from lignocellulose[28] and is a potential alternative biofuel[29]. Cyclopentane, on the other hand, is a
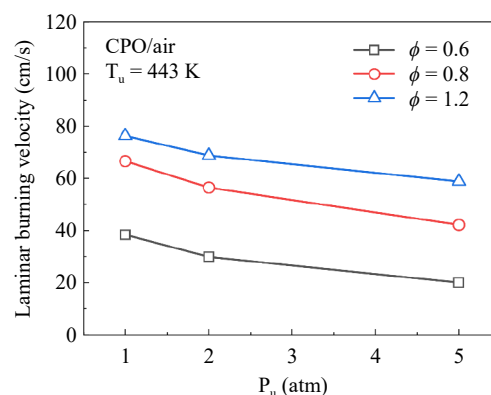

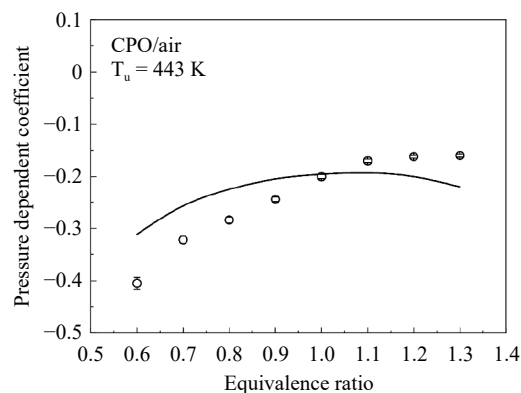**Fig. 7** Measured LBVs of cyclopentanone/air mixtures at 443 K, $\phi = 0.6$, 0.8, and 1.2.

Fig. 6 Measured and simulated LBVs for cyclopentanone/air mixtures.

Fig. 8 Measured (symbols) and simulated (lines) pressure dependent coefficient β for cyclopentanone/air flame.
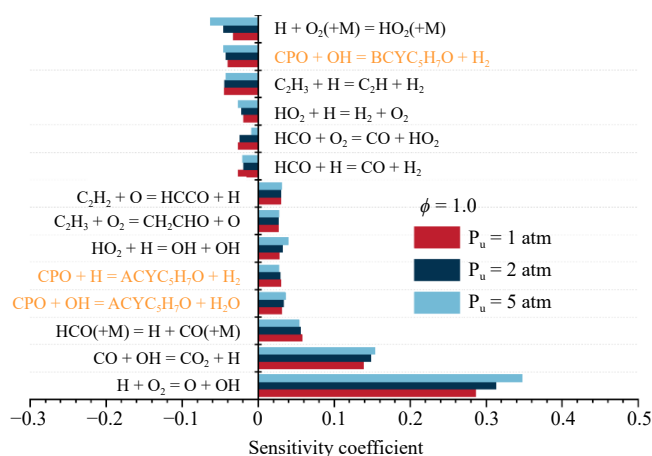
Fig. 9 Sensitivity analysis of LBV for cyclopentanone/air mixtures at $\phi = 1.0$ and various pressures.

five-membered cyclic alkane recognized as a high-octane alternative fuel. In this work, the LBVs of the three cyclic fuels with similar five-membered ring structures, namely cyclopentanone, cyclopentanol, and cyclopentane, are further compared to investigate the effect of various functional groups in the cyclic fuels on the flame propagation. However, no experimental data on the LBVs of cyclopentanol and cyclopentane at 443 K has been reported in the literature. To enable a direct comparison, simulated LBV values under the same conditions are used in this work. It is important to note that the kinetic models of cyclopentane and cyclopentanol are derived from the works of Zhao et al.[30] and Cai et al.[29,31], respectively, both of which have been validated against LBV experimental data.

Figure 10 shows a comparison of the simulated LBVs for the three fuels at 443 K and 1 atm. It can be seen that cyclopentanone flame propagates fastest, followed by cyclopentanol, with cyclopentane showing the slowest flame propagates. The maximum LBVs for all three fuels occur near $\phi = 1.1$, with the LBV of cyclopentanone at 80.2 cm/s, while the LBV of cyclopentanol and cyclopentane at 73.2 and 67.0 cm/s, respectively. Further analysis is carried out to gain insight into the control mechanisms behind this discrepancy. Notably, thermal effects are a significant factor influencing flame propagation. The adiabatic flame temperatures for the three fuels were calculated at the same conditions, as shown in Fig. 11. These temperatures are similar, with a difference of less than 20 K. Cyclopentanol exhibits a marginally lower flame temperature compared to the other two fuels. Additionally, the molecular weights of
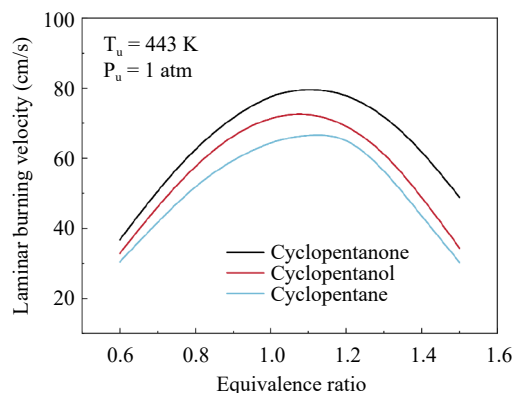
the three fuels are also comparable, resulting in similar transport properties. Therefore, it can be inferred that the chemical effect is the main reason for the significant difference in the flame propagation among the three fuels. This difference is mainly attributed to the fuel molecular structure, which affects the pool of radicals in their combustion process.

The ROP analysis showed that the initial consumption pathways for all three cyclic fuels involve H-abstraction with O_2 and various radicals, leading to the formation of fuel radicals. Figure 12 shows the C-H bond dissociation energies (BDE) at various carbon sites for the three fuel molecules. Cyclopentane, a symmetric molecule, exhibits a uniform C-H BDE of 97.1 kcal/mol. In cyclopentanol, the hydroxyl group induces a weakening effect on the C-H bond on the α-carbon, reducing its BDE by 4 kcal/mol compared to cyclopentane, while the C-H BDEs at the β-carbon and γ-carbon remain consistent with those of cyclopentane. In cyclopentanone, the C-H bond dissociation energy on the β-carbon is significantly lower than the corresponding sites in cyclopentane and cyclopentanol due to the substitution of the carbonyl group, with a value of only 90.3 kcal/mol. As a result, for the initial consumption of the three fuels, cyclopentanone is the most susceptible to H-abstraction, followed by cyclopentanol, and then cyclopentane.

As mentioned above, cyclopentanone generates intermediates such as ethylene, vinyl, and 1,3-butadiene through reaction pathways such as H-abstraction, ring opening, and β-dissociation. For cyclopentanol, the reaction network is more complex, it undergoes H-abstraction at three different carbon sites, producing fuel radicals including α-cyclopentanol, β-cyclopentanol, and γ-cyclopentanol. Specifically, α-cyclopentanol mainly reacts with oxygen to form stable cyclopentanone. β-cyclopentanol and γ-cyclopentanol are mainly consumed through hydrogenation to form cyclopentenol, followed by H-abstraction, ring-opening, and β-dissociation reactions to form small products such as C_3H_3, C_2H_3OH, etc. For cyclopentane, H-abstraction initially produces cyclopentyl, most of which undergoes ring-opening reactions to form n-pentenyl, with a
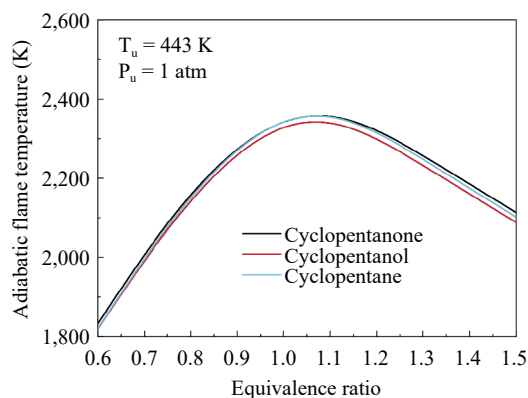

Fig. 11 Calculated adiabatic flame temperatures for cyclopentanone, cyclopentanol, and cyclopentane at 1 atm and 443 K.

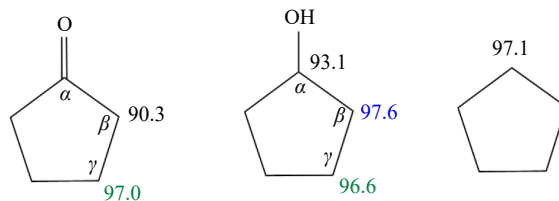**Fig. 10** Simulated LBVs of cyclopentanone, cyclopentanol[29,31], and cyclopentane[30] at 1 atm and 443 K.

Fig. 12 C-H BDE (kcal/mol) of cyclopentanone[9], cyclopentanol[29], and cyclopentane[29] at 298 K.

small fraction undergoing hydrogenation to form cyclopentene. It should be noted that the *n*-pentenyl undergoes subsequent β-scission reaction to form 1,3-butadiene and CH_3. This indicates that cyclopentane flames produce a significant amount of CH_3, whereas cyclopentanone and cyclopentanol flames generate relatively lower amounts of CH_3.

Figure 13 shows the maximum concentrations of the four critical radicals associated with flame propagation at $T_u = 443$ K, $P_u = 1$ atm, and $\phi = 1.1$. Among these, H and OH are the primary reactants in fuel H-abstraction reactions and critical intermediates influencing flame propagation. As show in Fig. 13, the maximum OH concentration for the three fuels is quite close, while the H concentration for cyclopentanone is significantly higher than the other two fuels. In addition, the CH_3 radical concentrations vary slightly among the three fuels. As previously mentioned, the intermediates in the cyclopentane flame are primarily CH_3 and allyl. As can be seen, cyclopentane has the highest peak concentration of CH_3 among the three fuels. CH_3 can consume H radicals through the chain-termination reaction $CH_3 + H (+ M) = CH_4 (+ M)$, thus inhibiting flame propagation. Therefore, the lower H radical concentration and higher CH_3 concentration inhibit the flame propagation of cyclopentane, which results in a significantly lower LBV than cyclopentanone and cyclopentanol. Additionally, the maximum C_2H_3 concentration in cyclopentanone is approximately twice that of cyclopentanol. From the ROP analysis (Fig. 4) and sensitivity analysis (Fig. 5), it can be seen that the C_2H_3 is an important intermediate in the cyclopentanone flame, readily undergoes the chain branching reactions, such as $C_2H_3 + O_2 = CH_2CHO + O$, which increases the reactivity and promotes flame propagation. The higher C_2H_3 concentration in cyclopentanone contributes to its higher LBV.

Conclusions

Laminar flame propagation of cyclopentanone/air mixtures was experimentally investigated using a constant-volume combustion vessel. Measurements of LBVs and Markstein lengths were conducted at initial pressures of 1, 2, and 5 atm and equivalence ratios ranging from 0.7–1.5, and an initial temperature of 443 K. The performance of three kinetic models in predicting experimental data was compared. Given the good predictions by the Li model, a detailed kinetic analysis was carried out to explore the chemical effect of the equivalence ratio and initial pressure on flame propagation. The main conclusions are drawn as follows:

(1) The LBVs of cyclopentanone show distinct pressure dependence, with increased pressure inhibiting the flame propagation. Under various pressures, the LBV increases and then decreases as the equivalence ratio rises, with the peak located at $\phi = 1.1$.
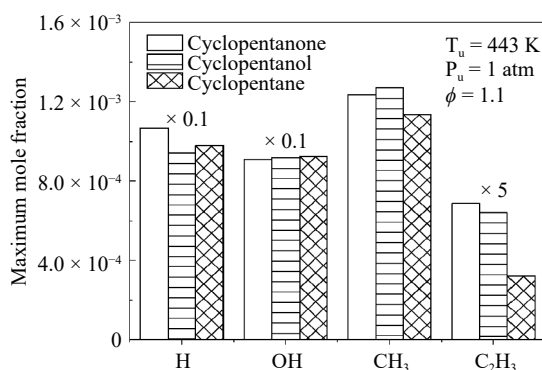

Fig. 13 Simulated maximum mole fraction of key radicals in cyclopentanone, cyclopentane, and cyclopentanol flames

(2) H-abstraction reactions of cyclopentanone are the primary pathways for fuel consumption. Vinyl-related reactions play a more significant role in cyclopentanone flames, with $C_2H_3 + H = C_2H_2 + H_2$ being the most critical inhibiting reaction under rich conditions. Under equivalent conditions, the sensitivity coefficient of $H + O_2 (+ M) = HO_2 (+ M)$ exhibits a gradually increase with rising initial pressure and exceeds that of $C_2H_3 + H = C_2H_2 + H_2$.

(3) A comparison of LBVs for cyclopentanone, cyclopentane, and cyclopentanol shows that cyclopentanone exhibits the fastest flame propagation. This behavior is mainly attributed to the carbonyl functional group in cyclopentanone, which promotes the generation of H and C_2H_3 radicals, further accelerating its flame propagation.

Author contributions

The authors confirm contribution to the paper as follows: data collection and analysis: Zhang Q, Fang J, Fang Q; formal analysis: Zhang Q, Fang J, Li W; writing – original draft: Zhang Q; writing – review & editing: Li W. All authors reviewed the results and approved the final version of the manuscript.

Data availability

The experimental and analytical data obtained in this study are included in this published article.

Conflict of interest

The authors declare that they have no conflict of interest.

References

1. Hronec M, Fulajtarová K. 2012. Selective transformation of furfural to cyclopentanone. *Catalysis Communications* 24:100−4
2. Yang Y, Dec JE. 2013. Bio-Ketones: Autoignition Characteristics and Their Potential as Fuels for HCCI Engines. *SAE International Journal of Fuels and Lubricants* 6:713−28
3. Pepiot-Desjardins P, Pitsch H, Malhotra R, Kirby SR, Boehman AL. 2008. Structural group analysis for soot reduction tendency of oxygenated fuels. *Combustion and Flame* 154:191−205
4. Tong Q, Chen H, He J, Su X, Wei Z, et al. 2021. Experimental studies of combustion and emission characteristics of diesel engine fueled with diesel/cyclopentanone blend. *Energy Reports* 7:6756−68
5. Bao X, Jiang Y, Xu H, Wang C, Lattimore T, et al. 2017. Laminar flame characteristics of cyclopentanone at elevated temperatures. *Applied Energy* 195:671−80
6. Zhang K, Capriolo G, Kim G, Almansour B, Terracciano AC, et al. 2020. Experimental and kinetic modeling study of laminar burning velocities of cyclopentanone and its binary mixtures with ethanol and *n*-propanol. *Energy & Fuels* 34:11408−16
7. Zhang K, Lokachari N, Ninnemann E, Khanniche S, Green WH, et al. 2019. An experimental, theoretical, and modeling study of the ignition behavior of cyclopentanone. *Proceedings of the Combustion Institute* 37:657−65

8. Sun W, Tao T, Liao H, Hansen N, Yang B. 2019. Probing fuel-specific reaction intermediates from laminar premixed flames fueled by two C5 ketones and model interpretations. *Proceedings of the Combustion Institute* 37:1699–707

9. Li W, Ye L, Fang Q, Zou J, Yang J, et al. 2021. Exploration on thermal decomposition of cyclopentanone: a flow reactor pyrolysis and kinetic modeling study. *Energy & Fuels* 35:14023–34

10. Wang G, Li Y, Yuan W, Zhou Z, Wang Y, et al. 2017. Investigation on laminar burning velocities of benzene, toluene and ethylbenzene up to 20 atm. *Combustion and Flame* 184:312–23

11. Kelley AP, Law CK. 2009. Nonlinear effects in the extraction of laminar flame speeds from expanding spherical flames. *Combustion and Flame* 156:1844–51

12. CHEMKIN-PRO 15112. 2011. Reaction Design: San Diego.

13. Yu H, Han W, Santner J, Gou X, Sohn CH, et al. 2014. Radiation-induced uncertainty in laminar flame speed measured from propagating spherical flames. *Combustion and Flame* 161:2815–24

14. de Vries J, Lowry WB, Serinyel Z, Curran HJ, Petersen EL. 2011. Laminar flame speed measurements of dimethyl ether in air at pressures up to 10atm. *Fuel* 90:331–38

15. Wang H, You X, Joshi AV, Davis SG, Laskin A, et al. 2007. *USC Mech Version II. High-temperature combustion reaction model of H2/CO/C1-C4 compounds*. https://ignis.usc.edu:80/Mechanisms/USC-Mech%20II/USC_Mech%20II.htm

16. Yuan W, Li Y, Dagaut P, Yang J, Qi F. 2015. Investigation on the pyrolysis and oxidation of toluene over a wide range conditions. I. Flow reactor pyrolysis and jet stirred reactor oxidation. *Combustion and Flame* 162:3–21

17. Zhou CW, Li Y, O'Connor E, Somers KP, Thion S, et al. 2016. A comprehensive experimental and modeling study of isobutene oxidation. *Combustion and Flame* 167:353–79

18. Serinyel Z, Chaumeix N, Black G, Simmie JM, Curran HJ. 2010. Experimental and chemical kinetic modeling study of 3-pentanone oxidation. *The Journal of Physical Chemistry A* 114:12176–86

19. Bradley D, Hicks RA, Lawes M, Sheppard CGW, Woolley R. 1998. The measurement of laminar burning velocities and markstein numbers for Iso-octane–Air and Iso-octane–n-Heptane–Air mixtures at elevated temperatures and pressures in an explosion bomb. *Combustion and Flame* 115:126–44

20. Ma S, Zhang X, Dmitriev A, Shmakov A, Korobeinichev O, et al. 2021. Revisit laminar premixed ethylene flames at elevated pressures: A mass spectrometric and laminar flame propagation study. *Combustion and Flame* 230:111422

21. Li W, Wang G, Li Y, Li T, Zhang Y, et al. 2018. Experimental and kinetic modeling investigation on pyrolysis and combustion of n-butane and i-butane at various pressures. *Combustion and Flame* 191:126–41

22. Mei B, Zhang J, Ma S, Li W, Dmitriev A, et al. 2023. Revisit flame chemistry of propene at elevated pressures: insight into pressure effects on chemical structure and laminar flame propagation. *Combustion and Flame* 251:112725

23. Li W, Zhang Y, Mei B, Li Y, Cao C, et al. 2019. Experimental and kinetic modeling study of *n*-propanol and *i*-propanol combustion: Flow reactor pyrolysis and laminar flame propagation. *Combustion and Flame* 207:171–85

24. Veloo PS, Egolfopoulos FN. 2011. Flame propagation of butanol isomers/air mixtures. *Proceedings of the Combustion Institute* 33:987–93

25. Mei B, Zhang X, Ma S, Cui M, Guo H, et al. 2019. Experimental and kinetic modeling investigation on the laminar flame propagation of ammonia under oxygen enrichment and elevated pressure conditions. *Combustion and Flame* 210:236–46

26. Goswami M, Derks SCR, Coumans K, Slikker WJ, de Andrade Oliveira MH, et al. 2013. The effect of elevated pressures on the laminar burning velocity of methane + air mixtures. *Combustion and Flame* 160:1627–35

27. Wang G, Li Y, Yuan W, Wang Y, Zhou Z, et al. 2018. Investigation on laminar flame propagation of *n*-butanol/air and *n*-butanol/O2/He mixtures at pressures up to 20 atm. *Combustion and Flame* 191:368–80

28. Li XL, Deng J, Shi J, Pan T, Yu CG, et al. 2015. Selective conversion of furfural to cyclopentanone or cyclopentanol using different preparation methods of Cu–Co catalysts. *Green Chemistry* 17:1038–46

29. Cai L, Kröger L, Döntgen M, Leonhard K, Narayanaswamy K, et al. 2019. Exploring the combustion chemistry of a novel lignocellulose-derived biofuel: cyclopentanol. Part I: quantum chemistry calculation and kinetic modeling. *Combustion and Flame* 210:490–501

30. Zhao H, Wang J, Cai X, Tian Z, Li Q, et al. 2018. A comparison study of cyclopentane and cyclohexane laminar flame speeds at elevated pressures and temperatures. *Fuel* 234:238–46

31. Cai L, Minwegen H, Kruse S, Daniel Büttgen R, Hesse R, et al. 2019. Exploring the combustion chemistry of a novel lignocellulose-derived biofuel: cyclopentanol. Part II: experiment, model validation, and functional group analysis. *Combustion and Flame* 210:134–44